Enhancing lifetime of wireless sensor networks using multiple data sinks

Amar Prakash Azad*

INRIA, 2004, Route de lucioles,
Sophia Antipolis Cedex, 06902 , France
Email: amar.azad@ieee.org
*Corresponding author

A. Chockalingam

Department of Electrical Communication Engineering,
Indian Institute of Science,
Bangalore 560012, India
Email: achockal@ece.iisc.ernet.in

Abstract: In this paper, we address the fundamental question concerning the limits on the network lifetime in sensor networks when *multiple base stations* (BSs) are deployed as data sinks. Specifically, we derive upper bounds on the network lifetime when *multiple* BSs are employed, and obtain optimum locations of the base stations that maximise these lifetime bounds. For the case of two BSs, we jointly optimise the BS locations by maximising the lifetime bound using genetic algorithm. Joint optimisation for more number of BSs becomes prohibitively complex. Further, we propose a suboptimal approach for higher number of BSs, *Individually Optimum* method, where we optimise the next BS location using optimum location of previous BSs. *Individually Optimum* method has advantage of being attractive for solving the problem with more number of BSs at the cost of little compromised accuracy. We show that accuracy degradation is quite small for the case of three BSs.

Keywords: wireless sensor networks; network lifetime; multiple base stations; optimum base station locations; energy efficiency.

Reference to this paper should be made as follows: Azad, A.P. and Chockalingam, A. (2011) 'Enhancing lifetime of wireless sensor networks using multiple data sinks', *Int. J. Sensor Networks*, Vol. 9, Nos. 3/4, pp.139–157.

Biographical notes: Amar Prakash Azad received MS in Electrical Communication Engineering from Indian Institute of Science, India, in 2006, and PhD at INRIA, France, in 2010. His research interest spans in energy efficiency related issues in wireless networks, optimal network resource management and application of game theory in wireless networks.

A. Chockalingam is a Professor at the Department of ECE, Indian Institute of Science (IISc), Bangalore, India. He is a recipient of the Swarnajayanti Fellowship from the Department of Science and Technology, Government of India. He is an editor of *IEEE Transactions on Wireless Communications*. He has served as editor of *IEEE Transactions on Vehicular Technology*, and Guest Editor of *IEEE JSAC* and *IEEE JSTSP*. He is a Fellow of the Institution of Electronics and Telecommunication Engineers, and a Fellow of the Indian National Academy of Engineering. His research interest lie in the area of wireless communications and networking.

1 Introduction

Recent advances in the area of wireless communications and embedded systems have enabled the development of small-sized, low-cost and low-power sensor nodes that can communicate over short distances wirelessly (Akyildiz et al., 2002). The processing and communication functions embedded in the sensor nodes essentially allow networking of these nodes, which in turn can facilitate sensing function to be carried out in remote/hostile areas. A network of sensor nodes can be formed by densely deploying a large number of sensor nodes in a given sensing area, from where the sensed data from the various nodes are transported to a monitoring station often located far away from the sensing area. The transport of data from a source node to the monitoring station can be carried out on a multihop basis, where other intermediate sensor nodes act as relay nodes. Thus, each sensor node, in addition to behaving as a source node, often needs to act as a relay node for data from other nodes in the network. The wireless sensor nodes are powered by finite-energy batteries (e.g. 1.2 V, < 0.5 AH

batteries). Being deployed in remote/hostile sensing areas, these batteries are not easily replaced or recharged. Thus, end of battery life in a node essentially means end of the node life, which, in turn, can result in a change of network topology or in the end of network life itself. Thus, the network lifetime has a strong dependence on the battery lifetime. Hence, efficient use of battery energy is crucial to enhance the network lifetime. Several energy-efficient techniques to increase network lifetime have been investigated and widely reported in the literature, e.g. improving energy efficiency using system partitioning (e.g. clustering of sensor nodes) (Heinzelman et al., 2002), low-duty cycle reception (e.g. sleep mode), dynamic voltage scaling (energy saving at device level) (Heinzelman et al., 2000), energy-efficient MAC protocols (energy saving at link layer) (Ye et al., 2002), energy-aware routing (energy saving at network layer) (Rodoplu and Meng, 1998; Chang and Tassiulas, 2000).

Apart from the conventional and widely studied energy-efficient techniques (energy-aware routing, MAC, etc.), an interesting approach that has been drawing much research attention recently is the use of *multiple data collection platforms (also referred to as data sinks or base stations)* to enhance the lifetime of sensor networks (Duarte-Melo et al., 2004; Azad, 2006). This approach is particularly suitable in scenarios where the data transport model is such that the raw data from sensor nodes need to be passed on to data collecting platforms (i.e. data sinks/base stations). These platforms can be deployed within the sensing area if the sensing area is easily accessible (e.g. pollution or traffic monitoring). On the other hand, in case of remote/hostile sensing areas (e.g. battlefield surveillance), these platforms are expected to be deployed only along the boundary of the sensing area or far away from it. Note that *raw* data transport model differs from data collection transport models. Unprocessed data is relayed in the former case, whereas data aggregations and processing (e.g. in Heinzelman et al., 2002) is done at the passing relay nodes. Both the above approaches target different end applications. In this work, we focus on the models where *raw* data transportation is considered and the data collectors are not allowed inside the surveillance region.

1.1 Why multiple base stations?

The usefulness of employing multiple base stations (BS) can be illustrated using Figure 1. Figure 1a shows a sensor network with one BS, B_1, deployed along the boundary of the sensing region $\mathcal{R}$. In Figure 1b, three BSs, B_1, B_2, B_3, are deployed along the boundary, and all these three BSs are allowed to act as data sinks. That is, each sensor node can send its data to any one of these three BSs (may be to the BS towards which the cost is minimum). Base stations can communicate among themselves to collate the data collected (energy is not a major concern in the communication between the BSs).

Suppose the routing is done as shown in Figure 1. In the single-BS scenario in Figure 1a, the sensor node 6 takes four hops to reach the BS B_1. However, in the three-BSs scenario in Figure 1b, node 6 can reach BS B_3 in just two hops. That is, by having more than one BS as data sinks, the average number of hops between data source-sink pairs can get reduced. This will reduce the energy spent by a given sensor node for the purpose of relaying data from other nodes towards the BS, which, in turn, can potentially result in increased network lifetime as well as in larger amount of data delivered during the network lifetime. Gandham et al. (2003), Azad and Chockalingam (2006), Azad and Kamruzzaman (2008), Kim et al. (2007) and Shi and Hou (2009) showed that employing multiple base stations indeed enhances the performance of a sensor network under various scenarios.

Figure 1 Multihop data transport to base stations: (a) single base station scenario, (b) multiple base stations scenario (see online version for colours)

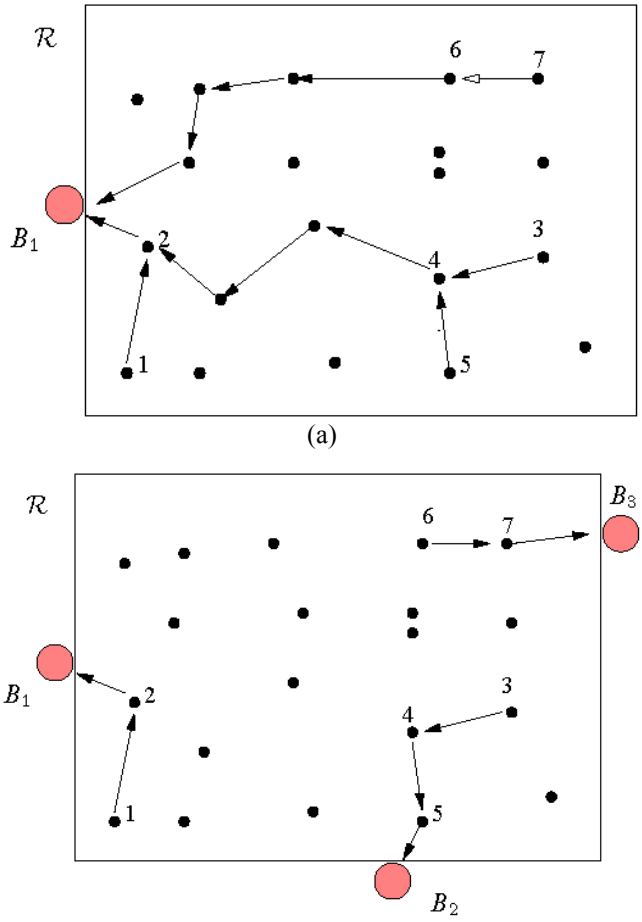

1.2 Our contribution

Our contribution in this paper is that we derive upper bounds on the lifetime of sensor networks with multiple BSs, taking into account the region of observation, number of nodes, number of BSs, locations of BSs, radio path loss characteristics, efficiency of node electronics, and energy available in each node. In addition, we obtain optimum locations of the BSs that maximise these lifetime bounds. For a scenario with single BS and a rectangular region of observation, we obtain closed-form expressions for the network lifetime bound and the optimum BS location. For the case of two BSs, we jointly optimise the BS locations by

maximising the lifetime bound using a genetic algorithm based optimisation. Joint optimisation for more number of BSs is complex. Hence, we propose a suboptimal approach for higher number of BSs, *Individually Optimum* method, where we optimise the next BS location using optimum location of previous BSs. For the case of three BSs, we optimise the third BS location using the previously obtained optimum locations of the first two BSs. We compare the accuracy of *Individually Optimum* method to that of *Joint Optimum* for the case of three BSs which is observed reasonably small. We also provide simulation results that validate the lifetime bounds and the optimum locations of the BSs.

1.3 Related work

Network lifetime has been a major topic of investigation in wireless sensor networks. Several papers have addressed the question of fundamental limits on the network lifetime (Bhardwaj et al., 2001; Ritter et al., 2005). In an early on paper in this topic, Bhardwaj et al. (2001) studied upper bounds on the lifetime of wireless sensor networks for data gathering with one data sink, where the network is considered to have life till the total energy in the network gets exhausted. In a later work, they extended their analysis by including data aggregation and network topology (Bhardwaj and Chandrakasan, 2002). Blough and Santi (2002) studied upper bounds on the lifetime of a network that employs a cell-based energy conservation technique under the hypothesis that nodes are distributed uniformly at random in a given region. Kalpakis et al. (in Blough and Santi, 2002) investigated the maximum lifetime data gathering problem, without and with data aggregation, assuming that each sensor node has the ability to transmit its packet to any other sensor node in the network or directly to the data sink. Zhang and Hou (2004) derived upper bounds on network lifetime when α-portion of the region only is required to be covered at any time. They derived these bounds for a given fixed node density in a finite region using the theory of coverage processes, assuming that the nodes are deployed as a Poisson point process. Hu and Li (2004) presented an asymptotic analysis on the operational lifetime of the network and the maximum sustainable throughput. Duarte-Melo et al. (2004) developed a fluid-flow model for maximising the lifetime, where they consider the active time for transmission and reception and ignore energy consumed in idle state and signalling-related overhead. An upper bound on the average network lifetime of a Code-Division Multiple Access (CDMA)-based system has been derived by Arnon (2005). While most of the above papers are concerned with the theoretical prediction of the limits on the network lifetime, Ritter et al. (2005) presented an interesting experimental evaluation of lifetime bounds, where they demonstrated the feasibility of a hardware approach to evaluate lifetime bounds.

We note that the lifetime studies in the above papers consider data gathering scenarios with only one data sink. More recently, there has been an increased interest in networks with multiple data sinks (Shah et al., 2003; Azad, 2006), with a motivation to enhance the network lifetime (e.g. see Figure 1 and the write-up associated with it in Section 1.1). Depending on the application and environment in which data gathering needs to be carried out, several scenarios are possible. Some scenarios of interest in the multiple data sinks approach include:

1 sinks are static and are allowed to be placed at the interior of the region to be sensed

2 sinks are mobile and are allowed to move within the interior of the region

3 sinks are static but are allowed to be placed only at the periphery/boundary of the region

4 sinks are mobile and are allowed to move only along the boundary.

For example, the *Data Mules* and *Message Ferrying* concepts investigated by Shah et al. (2003) and Zhao et al. (2004), respectively, essentially belong to Scenario 2, where mobile entities (called mules/ferries) move close to sensors, collect data from sensors (using a much lesser transmit power from the sensors because of the physical proximity between the mule/ferry and the sensors) and drop off the collected data to a central station. In a pollution monitoring application, for instance, the role of the mules/ferries can be carried out by cars/buses fitted with wireless transceivers. The mule/ferry can move on a specified route (e.g. campus shuttle route in a university campus) and collect/exchange messages with nodes when the mule/ferry comes close to the nodes. Network lifetime can be improved here because the sensor nodes need to spend less energy for transmission. Some degradation in delay performance is likely since the nodes have to wait till a mule/ferry comes near. Likewise, the Two-Tier Data Dissemination (TTDD) architecture using multiple mobile data sinks investigated by Luo et al. (2003) also belongs to Scenario 2. Das and Dutta (2005) also considered a Scenario 2 multiple data sink setting, and obtained analytical results for communication-energy savings for uniform random placement of data sinks as well as for a deterministic grid-based placement of sinks.

Scenario 3 is also of immense interest, particularly in applications where the sensing area is hostile (e.g. sensing in battlefield environment) or not easily accessible (e.g. wildlife tracking). In such situations, while the sensor nodes may be easily distributed in the sensing region, the data sink can be placed only along the boundary of the region. This is the motivating scenario for the work of Gandham et al. (2003), where the problem is to optimally deploy multiple data sinks along the boundary of the sensing region. They formulated the problem of choosing locations for the data sinks as an optimisation problem, which they solved using an integer linear program. Low-complexity heuristics for this problem have been presented by Azad and Chockalingam (2006). Wu and Chen (2007) showed that multiple data sinks are beneficial by the formation of smaller sub-networks with a data sink in each sub-network. It is shown that the performance of the entire network is enhanced when the performance of each partition

of the network is individually optimised. Optimal placement of data collectors in a 3D spatial setting is studied by Alsalih et al. (2008).

Our present work in this paper is primarily rooted in the multiple data sink approach of Scenario 3 in the above, for which lifetime bounds have not been reported. Accordingly, we derive upper bounds on the lifetime for the case of multiple data sinks following a similar analytical approach employed by Bhardwaj et al. (2001) for the single data sink case. We present analytical and simulation results that illustrate the lifetime gain in the multiple data sink approach and the optimal placement of sinks in a Scenario 3 setting.

The rest of the paper is organised as follows. The system model is presented in Section 2. In Section 3, we derive lifetime upper bounds and optimum locations of BSs. Detailed derivations are moved to the Appendices. Simulation results and discussions are presented in Section 4. Conclusions are given in Section 5.

2 System model

2.1 Network

We consider a sensor network comprising of sensor nodes distributed in a rectangular region of observation $\mathcal{R}$. The nodes are capable of sensing and sending/relaying data to a BS or a set of BSs using multihop communication. We assume that K BSs are deployed along the periphery of the region of observation to collect data from the nodes. Each node performs sensing operation using an integrated sensing device attached to it, generates information out of it, and processes this information to produce data. It is this data which needs to be sent to the BS(s). At any given time, the nodes are characterised as dead or alive depending on the energy left in their batteries as being below or above a usable threshold. Live nodes participate in sensing as well as sending/relaying data to the BS(s). While relaying data as an intermediate node in the path, the node simply forwards the received data without any processing.

2.2 Node energy behaviour

Each node has a sensor, analog pre-conditioning and data conversion circuitry (A/D), digital signal processor and a radio transceiver (Chandrakasan et al., 1999; Bhardwaj et al., 2001). The key energy parameters are the energies needed to: (a) sense a bit (E_{sense}); (b) receive a bit (E_{rx}); and (c) transmit a bit over a distance d (E_{tx}). Assuming a d^{η} path loss model, where η is the path loss exponent (Stuber, 1997)

$$E_{tx} = \alpha_{11} + \alpha_2 d^{\eta}, \quad E_{rx} = \alpha_{12}, \quad E_{sense} = \alpha_3, \tag{1}$$

where α_{11} is the energy/bit consumed by the transmitter electronics, α_{12} is the energy/bit consumed by the receiver electronics, α_2 accounts for energy/bit dissipated in the transmit amplifier, and α_3 is the energy cost of sensing a bit (Bhardwaj et al., 2001). Typically E_{sense} is much small compared to E_{tx} and E_{rx}. The energy/bit consumed by a node acting as a relay that receives data and then transmits it d metres onward is

$$E_{\text{relay}}(d) = \alpha_{11} + \alpha_2 d^{\eta} + \alpha_{12} = \alpha_1 + \alpha_2 d^{\eta}, \tag{2}$$

where $\alpha_1 = \alpha_{11} + \alpha_{12}$. If r is the number of bits relayed per second, then energy consumed per second (i.e. power) is given by

$$P_{\text{relay}}(d) = r\, E_{\text{relay}}(d). \tag{3}$$

We will use the following values for the energy parameters which are reported in the literature (Heinzelman, 2000; Bhardwaj et al., 2001): α_1 = 180 nJ/bit and α_2 = 10pJ/bit/m^2 (for $\eta = 2$) or 0.001pJ/bit/m^4 (for $\eta = 4$).

2.3 Battery and network life

Each sensor node is powered by a finite-energy battery with an available energy of E_{battery} Joules at the initial network deployment. A sensor node ceases to operate if its battery is drained below a certain energy threshold (i.e. available energy goes below some usable threshold). Often, network lifetime is defined as the time for the first node to die (Heinzelman et al., 2002; Chang and Tassiulas, 2000; Bhardwaj et al., 2001; Blough and Santi, 2002) or as the time for a certain percentage of network nodes to die (Xu et al., 2001). As by Heinzelman et al. (2002), Chang and Tassiulas (2000), Bhardwaj et al. (2001), Blough and Santi (2002), we also define network lifetime as the time for the first node to die. Given the region of observation ($\mathcal{R}$), number of nodes (N), initial energy in each node (E_{battery}), node energy parameters (α_1, α_2, α_3), path loss parameters (η), we are interested in (a) deriving bounds on the network lifetime when K, $K \geq 1$ BSs are deployed as data sinks along the periphery of the observation region, and (b) obtaining optimal locations of these BSs.

2.4 Minimum energy relay

The bounding of network lifetimes often involves the problem of establishing a data link of certain rate r between a transmitter (A) and a receiver (B) separated by distance D metres. This can be done either by directly transmitting from A to B (single hop) or by using several intermediate nodes acting as relays (multihop). A scheme that transports data between two nodes such that the overall rate of energy dissipation is minimised is called a *minimum energy relay* (Bhardwaj et al., 2001). If $M-1$ relays are introduced between A and B, i.e. M links between A and B (Figure 2), the overall rate of dissipation is given by

$$P_{\text{link}}(D) = \sum_{i=1}^{M} P_{\text{relay}}(d_i) - r\alpha_{12}, \tag{4}$$

where d_i is the inter-node distance of the i-th link. In equation (4), $r\ \alpha_{12}$ is subtracted to account for the fact that the source node A need not spend any energy for receiving.

Figure 2 $M-1$ relay nodes between points A and B

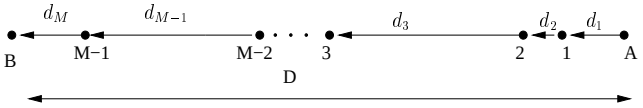

The following minimum energy relay theorem given by Bhardwaj et al. (2001) is relevant in the lifetime derivation for multiple BSs scenario.

Minimum Energy Relay Theorem: *Given D and the number of intermediate relays (M−1), $P_{link}(D)$ is minimised when all hop distances (i.e. d_i's) are made equal to D/M. This result holds for all radios with convex power versus distance curves, i.e. whose energy per bit is a convex function of the distance over which the bit is transmitted.*

The above theorem has been proved using Jensen's inequality in Bhardwaj et al. (2001). From the above and equation (4), it can be seen that the optimum number of hops (links) is the one that minimises $MP_{\text{relay}}(D/M)$, and is given by

$$M_{opt} = \left\lfloor \frac{D}{d_{\text{char}}} \right\rfloor \ \text{or} \ \left\lfloor \frac{D}{d_{\text{char}}} \right\rfloor, \tag{5}$$

where the distance d_{char} is given by

$$d_{\text{char}} = \sqrt[\eta]{\frac{\alpha_1}{\alpha_2(\eta-1)}}. \tag{6}$$

Equations (5) and (6) can be shown by substituting $d_i = D/M$, $i = 1, \ldots, M$ in equation (4), and differentiating it w.r.t. M and equating to zero, i.e. differentiating $P_{\text{link}}(D) = MP_{\text{relay}}(\frac{D}{M}) - r\alpha_{12} = rM(\alpha_1 + \alpha_2(\frac{D}{M})^{\eta}) - r\alpha_{12}$, w.r.t. M and equating to zero gives equations (5) and (6). This result says that, for a given distance D, there is an optimum number of relay nodes ($M_{opt} - 1$); using more or less than this optimal number leads to energy inefficiencies. Hence, a bound on the energy dissipation rate of relaying a bit over distance D can be obtained by substituting $M = \frac{D}{d_{\text{char}}}$ in the link power expression $MP_{\text{relay}}(\frac{D}{M}) - r\alpha_{12}$, i.e.

$$\begin{aligned} P_{\text{link}}(D) &\geq r\frac{D}{d_{\text{char}}}P_{\text{relay}}(d_{\text{char}}) - r\alpha_{12} \\ &= \left(\frac{D}{d_{\text{char}}}(\alpha_1 + \alpha_2 d_{\text{char}}^{\eta}) - \alpha_{12}\right)r \\ &= \left(\frac{D}{d_{\text{char}}}\alpha_1\frac{\eta}{\eta-1} - \alpha_{12}\right)r, \end{aligned} \tag{7}$$

with equality if and only if D is an integral multiple of d_{char}. From the minimum energy relay argument above, the actual power dissipated in the network (P_{nw}) is always larger than or equal to the sum of this $P_{\text{link}}(D)$ and the power for sensing, i.e.

$$\begin{aligned} P_{\text{nw}}(D) &\geq P_{\text{link}}(D) + P_{\text{sense}} \\ &\geq \left(\alpha_1\frac{\eta}{\eta-1}\frac{D}{d_{\text{char}}} - \alpha_{12}\right)r + \alpha_3 r. \end{aligned} \tag{8}$$

As an approximation, the sensing power can be ignored since the power for relaying data dominates.

Remark: *Note that the above theorem states that the minimum energy spent from a node over a distance D is a linear function of D, i.e. $P_{\text{nw}}(D) = L(D)$ (ignoring the sensing energy consumption). Here, we denote by L(.) a linear function.*

3 Bounds on network lifetime

Our goal is to obtain upper bounds on network lifetime. In this section, we derive network lifetime upper bounds and the corresponding optimal locations of the BSs which achieve the bounds. To start with, we take up the single BS case, state the problem formulation, and obtain the lifetime upper bound. We illustrate the numerical results by taking a rectangular network region. Though we illustrate the results for rectangular network region, we conjecture that the formulation is general enough and can be applied for any convex network region. We understand that a convex network region would be able to cover a large class of practical network scenarios. We then proceed to the multiple BSs scenario, where the problem becomes more complex. We present our main contribution, the approach of network partitioning, which enables us to deal with multiple BSs.

3.1 Single base station

Consider a region of observation $\mathcal{R}$ with nodes uniformly distributed. Let the BS be located at point $\sigma \in Bo(\mathcal{R})$ where $Bo(\mathcal{R})$ denotes the set of points which encloses the region $\mathcal{R}$. In other words, $Bo(\mathcal{R})$ denotes the boundary line of the network region. The minimum energy spent by a node located at point ξ in the network is given by $P_{\text{nw}}(D(\xi, \sigma))$, where $D(\xi, \sigma)$ denotes the distance between node location ξ to the BS location σ. Consider that N nodes are uniformly distributed in the network region and the node density can be approximated by a continuous r.v. $\rho(.)$, which is function of location ξ. Thus, the minimum energy spent over the entire network region can be given by

$$P_{\text{NW}}^{(\sigma)} = N\int\int_{\mathcal{R}} P_{\text{nw}}(D(\xi,\sigma))\rho(\xi)d\xi. \tag{9}$$

Note that $P_{\text{NW}}^{(\sigma)}$ is a function of BS location σ. Without loss of generality, $P_{\text{NW}}^{(\sigma)}$ corresponds to one unit of data (e.g. 1 bit). Therefore, the network lifetime bound can be stated by the following lemma.

Lemma 1: *The upper bound on the network lifetime for single BS and the optimal location of the BS are given by*

$$\mathcal{T}_{one-BS}^{*} = \max_{\sigma \in Bo(\mathcal{R})} \frac{NE_{battery}}{P_{NW}^{(\sigma),}} \tag{10}$$

$$\sigma^{*} = \arg\max_{\sigma \in Bo(\mathcal{R})} \frac{NE_{battery}}{P_{NW}^{(\sigma)}}. \tag{11}$$

Proof: Let $T_{\text{one-BS}}^{(\sigma)}$ denote the time until the first node dies (the network lifetime) for a given BS location σ. Achieving maximum network lifetime of a given network can be no greater than the total energy in the network at the beginning, i.e. $NE_{battery}$. Thus, we have

$$P_{\text{NW}}^{(\sigma)} T_{\text{one-BS}}^{(\sigma)} \leq NE_{\text{battery}}. \tag{12}$$

Therefore, given the BS location σ, the bound on network lifetime is given by

$$\mathcal{T}_{\text{one-BS}}^{(\sigma)} = \frac{NE_{\text{battery}}}{P_{\text{NW}}^{(\sigma)}}. \tag{13}$$

The upper bound on the entire network lifetime can thus be given by simple maximisation over BS locations,

$$\mathcal{T}_{\text{one-BS}}^{*} = \max_{\sigma \in Bo(\mathcal{R})} \mathcal{T}_{\text{one-BS}}^{(\sigma)} = \max_{\sigma \in Bo(\mathcal{R})} \frac{NE_{\text{battery}}}{P_{\text{NW}}^{(\sigma)}}$$

$$\sigma^{*} = \arg\max_{\sigma \in Bo(\mathcal{R})} \mathcal{T}_{\text{one-BS}}^{(p)} = \arg\max_{\sigma \in Bo(\mathcal{R})} \frac{NE_{\text{battery}}}{P_{\text{NW}}^{(\sigma)}}.$$

We express the network lifetime bound by the following alternate notation

$$\mathcal{T}_{\text{one-BS}}^{*} = \mathcal{T}_{\text{one-BS}}^{(\sigma^{*})}.$$

3.1.1 Single BS in rectangular network region

Let L and W denote the length and width of the rectangular network region, as shown in Figure 3. Let us denote all the four sides of the rectangular region as follows: $\underline{X}$ denotes the side from (0, 0) to (L, 0), $\overline{X}$ denotes the side from (0, W) to (L, W)), $\underline{Y}$ denotes the side from (0, 0) to (0, W), and $\overline{Y}$ denotes the side from (L, 0) to (L, W)). The BS B_1 can be located on any one of these four sides. Consider the following scenarios of BS placement:

- L-side: when the BS is placed either on the side $\underline{X}$ or on the side $\overline{X}$.
- W-side: when the BS is placed either on the side $\underline{Y}$ or on the side $\overline{Y}$.

Figure 3 Single base station placements: (a) B_1 located on W-side, (b) B_1 located on L-side (see online version for colours)

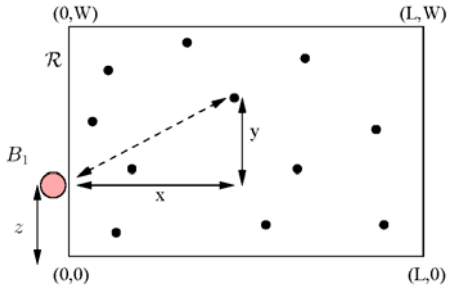

a) B_1 located on W-side

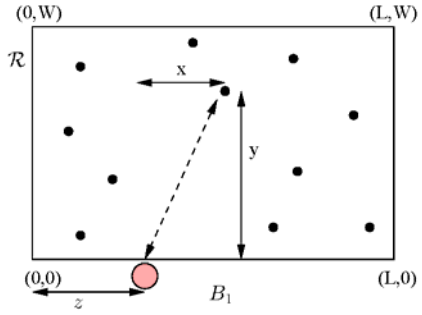

b) B_1 located on L-side

Let B_1 be located at a distance of z from the origin on the y-axis as shown in Figure 3a. Consider a source node in $\mathcal{R}$ at a distance of $D' = \sqrt{x^2 + y^2}$ from B_1. Denoting the energy dissipation in the entire network for a given BS location at distance z by $P_{\text{NW}}^{(z)}$, and assuming uniform distribution of N nodes, we study the lifetime bound in the following.

Proposition 1: *For a given rectangular network region $\mathcal{R}$ with length L and width $W < L$, and uniformly distributed sensor nodes with density ρ, the upper bound on the network lifetime $\mathcal{T}^{*}$ for single BS is given by*

$$\mathcal{T}^{*} = \frac{NE_{battery}}{r\alpha_1 \frac{\eta}{\eta - 1} \frac{d_{\text{one-BS}}(\sigma^{*})}{d_{char}}}, \tag{14}$$

and the optimal BS location σ^{*} is given as

$$\sigma^{*} = \left(0, \frac{\text{W}}{2}\right) \text{ or } \left(L, \frac{W}{2}\right), \tag{15}$$

where

$$d_{one-BS}(\sigma^{*}) = \frac{N}{12WL}\Big[2WL\sqrt{(4L^2 + W^2)} - \frac{W^3}{2}\ln(W/2) + \frac{3W^3}{8}\ln\left(L + \sqrt{(L^2 + W^2/4)}\right) + 2L^3 \ln\left(W/2 + \sqrt{(L + W^2/4)}\right)\Big]. \tag{16}$$

Proof: Considering the rectangular region as shown in Figure 3, the BS can be on any side of $\mathcal{R}$. Let the coordinates be taken as in Figure 3. Considering the side $\underline{Y}$, i.e. (0, 0) to (0, W), let the distance of BS location from the

origin be denoted by z. From equation (9), the minimum energy spent over the network can be given by

$$P_{\mathrm{NW}}^{(z)} = N\int\int_{\mathcal{R}} P_{\mathrm{nw}}(x,y)\frac{1}{WL}dx\,dy. \tag{17}$$

By the minimum energy relay argument, it is seen that $P_{\mathrm{nw}}(x,y) \geq P_{\mathrm{link}}\left(\sqrt{x^2+y^2}\right)$, and hence

$$\begin{aligned} P_{\mathrm{NW}}^{(z)} &\geq \frac{N}{WL}\int_{-z}^{W-z}\int_{0}^{L} P_{\mathrm{link}}\left(\sqrt{x^2+y^2}\right)dx\,dy \\ &= r\alpha_1\frac{\eta}{\eta-1}\frac{N}{WL}\int_{-z}^{W-z}\int_{0}^{L}\frac{\sqrt{x^2+y^2}}{d_{\mathrm{char}}}dx\;dy \\ &= r\alpha_1\frac{\eta}{\eta-1}\frac{d_{\text{one-BS}(z)}}{d_{\mathrm{char}}}, \end{aligned} \tag{18}$$

where

$$\begin{aligned} d_{\text{one-BS}}(z) &= \frac{N}{WL}\int_{-z}^{W-z}\int_{0}^{L}\sqrt{x^2+y^2}\,dx\,dy \\ &= \frac{N}{12WL}\Bigg(4L_z\sqrt{L^2+z^2}+4L(W-z)\sqrt{L^2+(W-z)^2} \\ &\quad -(W-z)^3\ln\left[\frac{(W-z)^2}{(L+\sqrt{L^2+(W-z)^2})^2}\right]-z^3 \\ &\quad \ln\left[\frac{z^2}{(L^2+\sqrt{L^2+z^2})^2}\right]+2L^3\ln\left[W-z+\sqrt{L+(W-z)^2}\right]\Bigg). \end{aligned} \tag{19}$$

The bound on the lifetime of network when the BS location is restricted to only $\underline{Y}$ can be expressed using Lemma 1, as

$$\mathcal{T}^{*}_{\text{one-BS}}(\underline{Y}) = \max_{z\in\underline{Y}}\frac{N\,E_{\mathrm{battery}}}{P_{\mathrm{NW}}^{(z)}} \tag{20}$$

$$z^{*}(\underline{Y}) = \arg\max_{z\in\underline{Y}}\frac{N\,E_{\mathrm{battery}}}{P_{\mathrm{NW}}^{(z)}}. \tag{21}$$

The above maximisation requires the computation of $\min_{z\in\underline{Y}} P_{\mathrm{NW}}^{(z)}$, which further needs the evaluation of the following maximisation problem, given by

$$z^{*}(\underline{Y}) = \arg\min_{z\in\underline{Y}} d_{\text{one-BS}}(z) = \arg\min_{z\in\underline{Y}}\int_{-z}^{W-z} M(y)\,dy,$$

where

$$\begin{aligned} M(y) &= \frac{1}{2}\Bigg[-\frac{1}{2}y^2\ln(y^2)+L\sqrt{(L^2+y^2)} \\ &\quad +y^2\ln(L+\sqrt{(L^2+y^2)})\Bigg]. \end{aligned} \tag{22}$$

The optimal value can be obtained from the basic derivative principle, i.e. by solving $M(W-z) - M(-z) = 0$, which yields $z = W/2$. For the second derivative test, it is simple to verify that the derivative of $M(z)$ at $z = W/2$ is positive; this confirms the optima to be minima. This concludes that

$$z^{*}(\underline{Y}) = W/2. \tag{23}$$

Substituting $z^{*}(\underline{Y}) = W/2$ in equation (19) gives a closed-form expression for $d_{\text{one-BS}}(z)$, which when substituted in equation (18) gives a closed-form expression for lifetime upper bound. In a similar way, the optimal BS location and the corresponding lifetime bound can be obtained for the BS placement on the side $\underline{X}$ (as in Figure 3b) as $z^{(\underline{X})}_{opt} = L/2$, and the corresponding lifetime bound is obtained by simply interchanging W and L in the lifetime bound equation. Due to symmetry, $\overline{X}$ corresponds to $\underline{X}$ and $\overline{Y}$ corresponds to $\underline{Y}$. It can be easily verified that $\mathcal{T}^{*}_{\text{one-BS}}(\underline{Y}) > \mathcal{T}^{*}_{\text{one-BS}}(\underline{X})$ for $L > W$. This concludes the proof.

A numerical example illustrating this observation is shown in Figure 4 for $L = 1000$ m, $W = 500$ m, and $E_{\mathrm{battery}} = 0.5$ J.

Figure 4 Normalised upper bound on network life time as a function of base station location for L = 1000 m, W = 500 m, single base station, and E_{battery} = 0.5 J

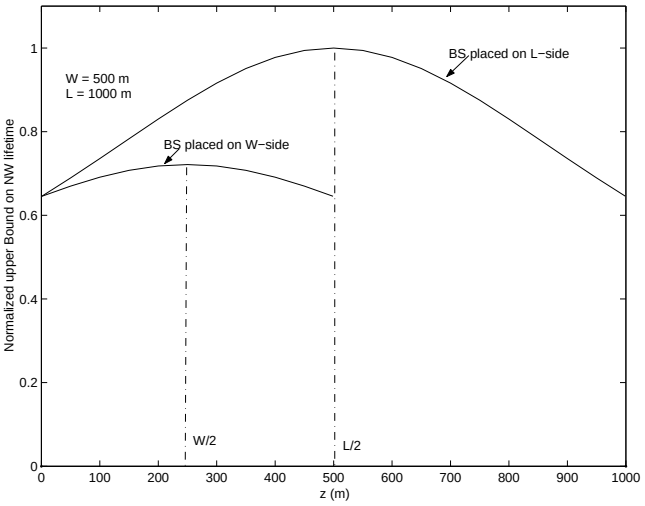

3.2 Multiple base stations

Deploying multiple BSs has been shown to be relatively more energy efficient because of reduced number of hops (Gandham et al., 2003). On the other hand, it brings more system complexity; e.g. a node should be transmitting to which BS, from an energy efficiency consideration (Azad and Chockalingam, 2006). It is learnt from the basic *minimum energy theorem* equation (8) that the transmission energy is proportional to the distance. This clearly indicates a node must transmit to the closest BS in order to spend minimum energy. This is a key point based on which we propose network partitioning method to obtain the upper bound on network lifetime in case of multiple BSs.

In this subsection, we introduce the network partitioning method and derive the upper bound on network lifetime. We illustrate the detailed procedure to compute the bound on network lifetime with two BSs for a rectangular region of network. We observe that solving the join optimisation problem of locating multiple BSs is of high complexity as the number of BSs grows. It becomes increasingly difficult to carry over the derivation for more than three BSs. We thus propose a suboptimal approach; an 'individual optimisation' method to derive the solution relatively easily but at the cost of little compromised accuracy. In order to study the performance of this suboptimal approach, we depict some comparative results between both the schemes.

3.2.1 Two base stations

Consider the case of two BSs, where the BSs B_1 and B_2 can be deployed in the following ways:

1 *Same side orientation (SSO):* Both BSs are on the same side as shown in Figure 5a. There are four such possibilities (i.e. both BSs can be deployed on any one of the four sides).

2 *Adjacent side orientation (ASO):* One BS each on adjacent sides as in Figure 5b. There are four such possibilities.

3 *Opposite side orientation (OSO):* One BS each on opposite sides as in Figure 5c. There are two such possibilities.

Figure 5 Placements of two base stations: (a) same side orientation, (b) adjacent side orientation, and (c) opposite side orientation (see online version for colours)

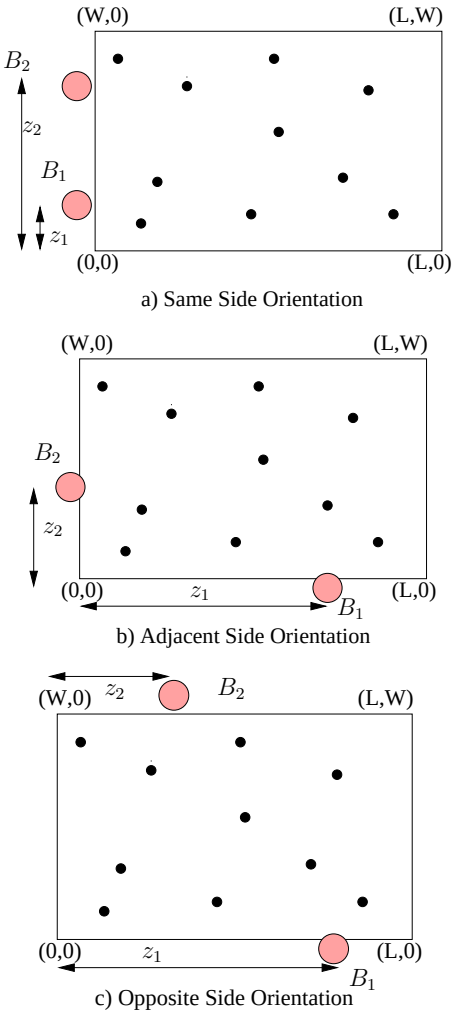

It is noted that, in order to jointly optimise the locations of B_1 and B_2, the network lifetime bounds for all the above possibilities of base station placement need to be derived. Due to the symmetry involved in the rectangular region considered, one possibility for each orientation only needs a new derivation. Accordingly, in the following, we present the derivation for the three different orientations as shown in Figure 5. Derivation for other possibilities follows similarly due to symmetry.

Each node in the network must be associated with any one BS. For each node, this can be done by choosing that BS towards which energy spent for delivering data from that node is minimum. From the minimum energy relay argument, the minimum energy spent is proportional to the distance D between source node and the BS [see RHS of equation (7)], and hence associating the node to its closest BS results in the least minimum energy spent. Accordingly, we associate each node with its closest BS. This results in the region $\mathcal{R}$ to be partitioned into two sub-regions $\mathcal{R}_1$ and $\mathcal{R}_2$ such that all nodes in sub-region $\mathcal{R}_1$ will be nearer to B_1 than B_2, and all nodes in sub-region $\mathcal{R}_2$ will be nearer to B_2 than B_1. It can be seen that this partitioning will occur along the perpendicular bisector of the line joining B_1 and B_2.

3.2.2 Derivation for Adjacent Side Orientation (ASO)

We first consider the derivation of network lifetime bound for the case of adjacent side orientation shown in Figure 5b, where B_1 is located on the x-axis at a distance of z_1 from the origin and B_2 is located on the y-axis at a distance of z_2 from the origin. The axis along which $\mathcal{R}_1$, $\mathcal{R}_2$ partition occurs depends on the locations of B_1 and B_2 (i.e. z_1 and z_2 in this case). For a given z_1 and z_2, the partition axis will belong to any one of the four possible axis types X_aX_b, X_aY_b, Y_aX_b and Y_aY_b as shown in Figure 6.

The partition axis can be represented by the straight line

$$Y = mX + c, \tag{24}$$

where $m = \frac{z_1}{z_2}$ and $c = \frac{z_2^2 - z_1^2}{2z_2}$. Then, from equation (24) we have

$$X_a = X\,|_{Y=0} \Rightarrow X_a = -\frac{C}{m} = \frac{z_1^2 - z_2^2}{2z_1}, \tag{25}$$

$$X_b = X\,|_{Y=W} \Rightarrow X_b = -\frac{W-c}{m} = \frac{Wz_2}{z_1} - \frac{z_2^2 - z_1^2}{2z_1}, \tag{26}$$

$$Y_a = Y\,|_{X=0} \Rightarrow Y_a = c = -\frac{z_2^2 - z_1^2}{2z_2}, \tag{27}$$

$$Y_b = Y\,|_{X=L} \Rightarrow Y_b = mL + c = \frac{Lz_1}{z_2} + \frac{z_2^2 - z_1^2}{2z_2}. \tag{28}$$

It is noted that for a given z_1 and z_2, the partition axis type is

1 X_aX_b if $X_a \geq 0$ and $X_b \leq L$ (Figure 6a)

2 X_aY_b if $X_a \geq 0$ and $Y_b \leq W$ (Figure 6b)

3 Y_aX_b if $Y_a \geq 0$ and $X_b \leq L$ (Figure 6c)

4 Y_aY_b if $Y_a \geq 0$ and $Y_b \leq W$ (Figure 6d).

Figure 6 Adjacent side orientation of two base stations. $\mathcal{R}_1$, $\mathcal{R}_2$ partition can occur along (a) X_aX_b axis, (b) X_aY_b axis, (c) Y_aX_b axis, and (d) Y_aY_b axis (see online version for colours)

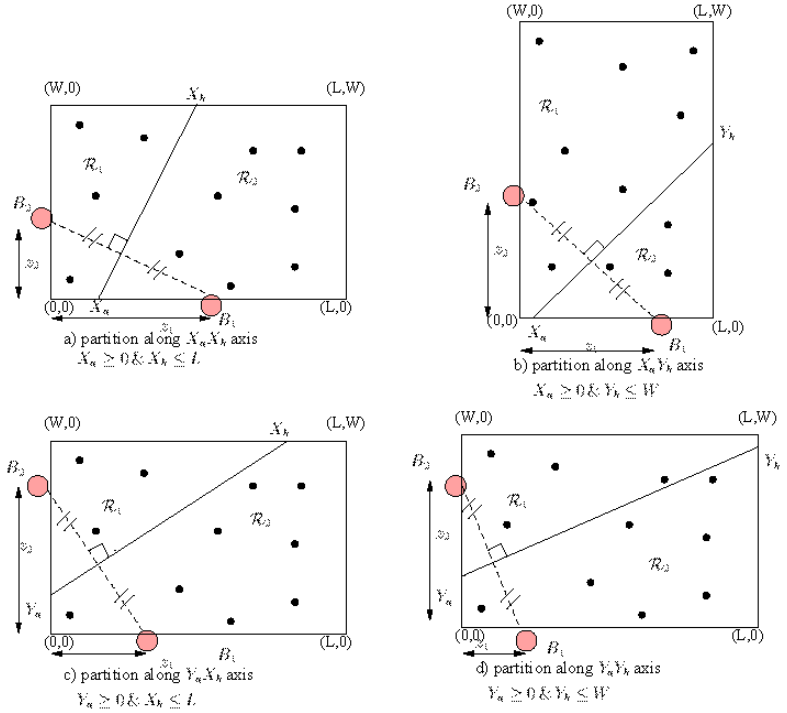

Now, the energy dissipation in the entire network with locations of BSs at distances z_1 and z_2 for the ASO case is given by

$$P_{\text{NW,aso}}^{(z_1,z_2)} = N\left(\iint_{\mathcal{R}_1} P_{\text{nw}}(x,y)\frac{1}{WL}dx\,dy + \iint_{\mathcal{R}_2} P_{\text{nw}}(x,y)\frac{1}{WL}dx\,dy\right) \tag{29}$$

By minimum energy relay argument, $P_{\text{nw}}(x,y) \geq P_{\text{link}}\left(\sqrt{x^2+y^2}\right)$, and hence

$$\begin{aligned} P_{\text{NW,aso}}^{(z_1,z_2)} &\geq \frac{N}{WL}\left(\iint_{\mathcal{R}_1} P_{\text{link}}\left(\sqrt{x^2+y^2}\right)dx\,dy + \iint_{\mathcal{R}_2} P_{\text{link}}\left(\sqrt{x^2+y^2}\right)dx\,dy\right) \\ &\geq \frac{r\alpha_1}{d_{\text{char}}}\frac{\eta}{\eta-1}\frac{N}{WL}\left(\iint_{\mathcal{R}1}\sqrt{x^2+y^2}\,dx\,dy + \iint_{\mathcal{R}_2}\sqrt{x^2+y^2}\,dx\,dy\right) \\ &\geq \frac{r\alpha_1}{d_{\text{char}}}\frac{\eta}{\eta-1}\frac{M}{WL}\left(d_{2-\text{BS,aso}}^{\mathcal{R}_1}(z_1,z_2) + d_{2-\text{BS,aso}}^{\mathcal{R}_2}(z_1,z_2)\right), \end{aligned} \tag{30}$$

where $d_{2-\text{BS,aso}}^{\mathcal{R}_1}(z_1,z_2)$ and $d_{2-\text{BS,aso}}^{\mathcal{R}_2}(z_1,z_2)$ are different for different partition axis types, and are of the form

$$d_{2-\text{BS,aso}}^{\mathcal{R}_1}(z_1,z_2) = \int_{y_1}^{y_2}\int_{x_1}^{x_2}\sqrt{x^2+y^2}\,dx\,dy + \int_{y_3}^{y_4}\int_{x_3}^{x_4}\sqrt{x^2+y^2}\,dx\,dy, \tag{31}$$

and

$$d_{2-\text{BS,aso}}^{\mathcal{R}_2}(z_1,z_2) = \int_{x_5}^{x_6}\int_{y_5}^{y_6}\sqrt{x^2+y^2}\,dy\,dx + \int_{x_7}^{x_8}\int_{y_7}^{y_8}\sqrt{x^2+y^2}\,dy\,dx. \tag{32}$$

Defining $X_{z_2} = X|_{Y=y+z_2}$ and $Y_{z_1} = Y|_{X=x+z_1}$ in equation (24), the values of the limits y_1, y_2,…, y_8 and x_1, x_2,…, x_8 in equations (31) and (32) for the various partition axis types in Figure 6 are tabulated in Table 1.

Table 1 Limits y_1, $y_2 \ldots y_8$ and x_1, $x_2 \ldots x_8$ in equations (31) and (32) for two base station ASO for various partition axis types in Figure 6

Limits	*For X_aX_b axis Figure 6a*	*For X_aY_b axis Figure 6b*	*For Y_aX_b axis Figure 6c*	*For Y_aY_b axis Figure 6d*
(x_1, x_2)	$(0, X_{z_2})$	$(0, X_{z_2})$	$(0, X_{z_2})$	$(0, X_{z_2})$
(y_1, y_2)	$(-z_2, W-z_2)$	$(-z_2, Y_b-z_2)$	(Y_a-z_2, Y_b-z_2)	$(Y_a-z_2, W-z_2)$
(x_3, x_4)	(0,0)	$(0, L)$	$(0, L)$	(0,0)
(y_3, y_4)	(0,0)	$(Y_b-z_2, W-z_2)$	$(Y_b-z_2, W-z_2)$	(0,0)
(x_5, x_6)	(X_a-z_1, X_b-z_1)	$(X_a-z_1, L-z_1)$	$(-z_1, L-z_1)$	$(-z_1, X_b-z_1)$
(y_5, y_6)	$(0, Y_{z_1})$	$(0, Y_{z_1})$	$(0, Y_{z_1})$	$(0, Y_{z_1})$)
(x_7, x_8)	$(X_b-z_1, L-z_1)$	(0,0)	(0,0)	$(X_b-z_1, L-z_1)$
(y_7, y_8)	$(0, W)$	(0,0)	(0,0)	$(0, W)$

Now, denoting $\mathcal{T}_{\text{2-BS,aso}}^{(z_1,z_2)}$ as the network lifetime with two BSs located at distances z_1, z_2 for the ASO case, we have

$$P_{\text{NW,aso}}^{(z_1,z_2)}\mathcal{T}_{\text{2-BS,aso}}^{(z_1,z_2)} \le N E_{\text{battery,}} \tag{33}$$

and hence an upper bound on lifetime for a given z_1 and z_2 and ASO can be obtained as

$$\mathcal{T}_{\text{2-BS,aso}}^{(z_1,z_2)} \le \frac{N E_{\text{battery}}}{\frac{r\alpha_1}{d_{char}}\frac{\eta}{\eta-1}\frac{N}{WL}\left(d_{\text{2-BS,aso}}^{\mathcal{R}_1}(z_1,z_2)+d_{\text{2-BS,aso}}^{\mathcal{R}_1}(z_1,z_2)\right)}. \tag{34}$$

The optimum BS locations for ASO case that maximises the above lifetime bound is then given by

$$\left(Z_1, opt, z_2, opt\right)_{\text{aso}} = \underset{z_2\in(0,W)}{\arg\max}\, z_1 \in (0,L),\ \mathcal{T}_{\text{2-BS,aso}}^{(z_1,z_2)}. \tag{35}$$

Following similar steps, the lifetime bounds for the cases SSO and OSO, $\mathcal{T}_{\text{2-BS,sso}}^{(z_1,z_2)}$ and $\mathcal{T}_{\text{2-BS,oso}}^{(z_1,z_2)}$, respectively, can be derived. These derivations are presented in Appendix A. Finally, the optimum locations of the BSs are chosen from the best locations of ASO, SSO and OSO cases, as

$$(z_1, \text{opt}, z_2, \text{opt}) = \underset{\substack{z_1\in(0,L),\\ z_2\in(0,\text{W})\\ \text{orient}\in\{\text{aso,sso,oso}\}}}{\arg\max}\ \mathcal{T}_{\text{2-BS,orient}}^{(z_1,z_2)}. \tag{36}$$

3.2.3 Numerical results for two base stations

The optimisation problem in equation (35) can be solved using known optimisation methods available in the literature. We have used a genetic algorithm (GA)-based optimisation because of its suitability for solving the objective function which involves non-linearity and multiple integrals. Also, if higher dimensions (more number of BSs) need to be tried with general distribution of nodes, GA could be a suitable approach. We evaluated the network lifetime upper bound and the optimum BS locations. The results thus obtained for SSO, ASO, and OSO cases are given in Table 2 for L = 1000 m, W = 500 m, and E_{battery} = 0.5 J. In the genetic algorithm, binary gene representation is used with Gene code length of 20 bits. The parameters for the genetic algorithm are: initial population = 20 bits, maximum number of generations = 10, mutation probability = 0.4, crossover probability = 0.8, number of independent runs = 10. The GA optimisation is performed for the specified region with L = 1000 m and W = 500 m.

Table 2 Upper bounds on network lifetime and optimal base station locations. Two base stations. Joint optimisation. L = 1000 m, W = 500 m, $E_{battery}$ = 0.5 J

Two Base Stations (Jointly Optimum)			
Orientation		*NW lifetime Upper Bound (# rounds)*	*Optimal locations of B_1, B_2*
SSO	W side	18.28	(0, 121.3), (0, 381.5)
	L side	31.36	(133.7, 0), (761.4, 0)
ASO		32.60	(693.2, 0), (0, 263.6)
OSO	W side	31.41	(0, 249.4), (1000, 251.2)
	L side	32.99	(716.6,0), (500, 282.6)

From the results in Table 2, it can be observed that the maximum lifetime bound occurs when the BSs are placed with opposite side orientation (OSO) on the L-side, and the corresponding coordinates of the optimum locations of B_1 and B_2 are (716.6 m, 0 m) and (500 m, 282.6 m). Thus, given the region of observation (in terms of W and L), initial battery energy (E_{battery}), path loss characteristics (η), and energy consumption behaviour of the node electronics (α_1, α_2), the above analysis allows us to compute an upper bound on the network lifetime and the corresponding optimum BS locations for the two BSs case.

3.3 Jointly optimum vs. individually optimum

It is noted that in the above optimisation procedure, the locations of B_1 and B_2 are jointly optimised. Though such joint optimisation is best in terms of performance, its complexity is high. Also, such joint optimisation will become prohibitively complex for more number of BSs. So, an alternate and relatively less complex solution is to individually optimise B_1 and B_2, i.e. fix the location of B_1 at the optimal location obtained from the solution of the one BS problem and find the optimal location for B_2 and the corresponding lifetime bound. We carried out such an individual optimisation for two BSs [by fixing BS B_1 at its individually optimum location (L/2, 0)], and the results of the optimisation are given in Table 3. From Table 3, it can be observed that, as expected, the individually optimised solution results in reduced lifetime bound compared to the jointly optimised solution (e.g. 31.41 rounds vs. 32.99 rounds for OSO). However, the individually optimised approach has the advantage of being attractive for solving the problem with more number of BSs. Like the jointly optimised solution, the individually optimised solution also results in the largest lifetime bound when the two BSs are deployed with opposite side orientation (OSO) on the L-side.

Table 3 Upper bounds on network lifetime and optimum base station locations for two base stations. B_1 fixed at optimum location obtained from solving single BS problem. L = 1000 m, W = 500 m, E_{battery} = 0.5 J

Two Base Stations (Individually Optimum)		
Location of B_1 fixed at (L/2,0) = (500,0)		
Orientation	*NW lifetime Upper Bound (#rounds)*	*Optimal location of B_2*
SSO	28.36	(164.9, 0)
ASO	30.22	(0, 496.2)
OSO	31.41	(502.5, 500)

3.4 Three base stations

As pointed out earlier, for the case of three BSs, jointly optimising the locations of B_1, B_2, B_3 can be prohibitively complex. Hence, in solving the three BSs problem, we take the approach of fixing the previously optimised locations of

B_1, B_2 obtained from the solution of two BSs problem, and then optimise the location of B_3. Once the BSs B_1 and B_2 are fixed, the problem gets simplified to optimising only over B_3 location.

Fixing B_1 and B_2 on the midpoints of opposite sides (which is the individually optimum two BS solution), B_3 can be located on any one of four sides. Placement of B_3 with Adjacent Side Orientation (ASO) and Same Side Orientation (SSO) as shown in Figure 7, respectively, need to be considered separately. In each of these AS and SS orientation possibilities, the region $\mathcal{R}$ is partitioned into sub-regions $\mathcal{R}_1$, $\mathcal{R}_2$, and $\mathcal{R}_3$. The partition occurs along the three axes which are the perpendicular bisectors of the lines connecting the three different BS pairs as shown in Figure 7. Proceeding in a similar way as done for the two BS problem, we have derived expressions for the upper bound on the network lifetime with three BSs. The derivation is given in Appendix B. These expressions were then optimised using genetic algorithm to compute the lifetime upper bound as well as the optimum location of B_3.

Figure 7 Placement of three base stations. B_1 and B_2 are placed at optimal locations obtained by solving the two base station problem. Location of B_3 is then optimised (a) B_3 on adjacent side of B_1. (b) B_3 on same side as B_1 (see online version for colours)

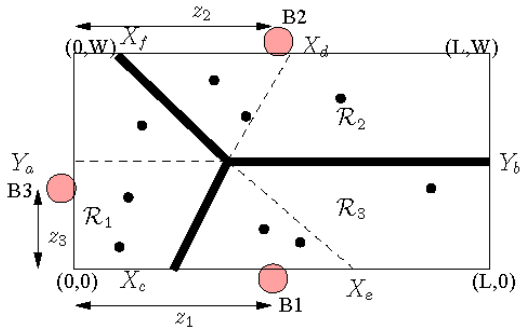

B_3 on adjacent side. $z_1 = z_2 = L/2$

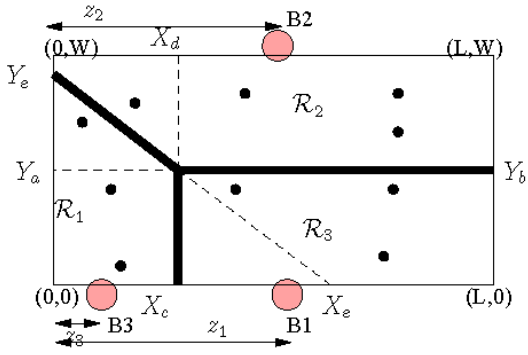

B_3 on same side. $z_1 = z_2 = L/2$

Table 4 shows the upper bound on the network lifetime computed for (a) SS orientation and (b) AS orientation. It can be seen that the AS orientation of B_3 results in a larger lifetime bound compared to SS orientation. The maximum lifetime bound for ASO is 38.38 rounds and the optimum location at which this maximum occurs is (0, 249.8).

Table 4 Upper bounds on network lifetime and optimum base station locations for three base stations. B_1 and B_2 fixed at optimum locations obtained from solving two base stations problem. L = 1000 m, W = 500 m, $E_{battery}$ = 0.5 J

Three Base Stations (Individually Optimum)		
Location of B_1 fixed at (500, 0) *Location of B_2 fixed at (500, 500)*		
Orientation	*NW lifetime Upper Bound (#rounds)*	*Optimum location of B_3*
SSO	36.44	(152.6, 0)
ASO	38.38	(0, 249.8)

Table 5 Compari son of the upper bounds on network lifetime for one, two, and three base stations. L = 1000 m, W = 500 m, $E_{battery}$ = 0.5 J

No. of BS	*NW lifetime Upper Bound (# rounds)*	*Optimum BS Locations*
One BS	24.34	B_1: (489.9, 0)
Two BS (Jointly opt)	32.99	B_1: (716.6, 0)
		B_2: (500, 282.6)
Two BS (Indiv. opt)	31.41	B_1: (500, 0)
		B_2: (502.5, 500)
Three BS (Indiv. opt)	38.38	B_1: (500, 0)
		B_2: (500, 500)
		B_3: (0, 249.8)

In Table 5, we present a comparison between the network lifetime bounds for one, two, and three BSs and their corresponding optimum BS locations. From Table 5, it can be observed that the lifetime bound increases for increasing number of BSs, as expected. For example, the lifetime bound is 24.3 rounds for one BS, whereas it gets increased to 38.4 rounds when three BSs are employed. The complexity of solving the problem for more than 3 BSs is high. So instead of giving the explicit lifetime results for 4 BSs or more, we looked at the average hop count between sensor nodes and their respective BSs as a function of number of BSs, which is easy to obtain through simulations. Figure 8 shows the average hop count as a function of number of BSs for L = 1000 m, W = 500 m, N = 50, averaged over 100 network realisations. From Figure 8, it can be seen that 4 BSs result in a reasonable reduction in average hop count compared to that of 3 BS. However, beyond 4 BSs the reduction in average hop count is not significant for the considered system scenario.

Figure 8 Average hop count between sensor nodes and their base stations as a function of number of base stations. L = 1000 m, W = 500 m, N = 50 nodes. 100 realisations of the network (see online version for colours)

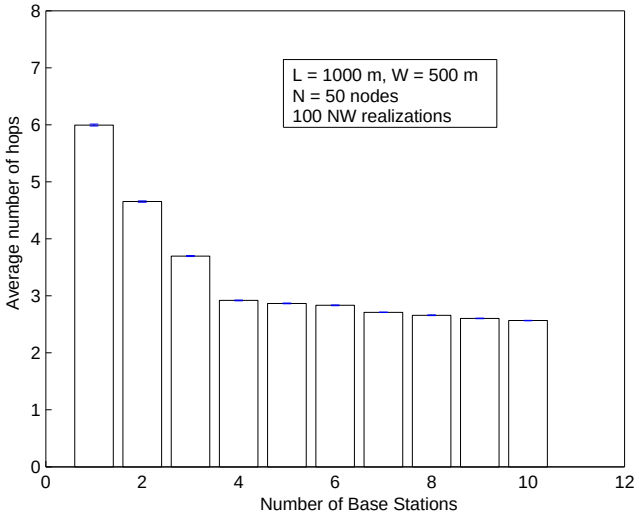

4 Simulation results

To validate the analytical bounds on the network lifetime, we carried out detailed simulations and obtained the simulated network lifetime over several network realisations at different BS locations. In the simulations, nodes are distributed uniformly in the rectangular region of observation $\mathcal{R}$ with L = 1000 m and W = 500 m. Different node densities in the network are considered by considering different number of nodes, namely N = 50 nodes. The transmission range of the sensor nodes is taken to be 250 m in the simulations. All nodes have an initial battery energy of 0.5 J. A modified version of the Minimum Cost Forwarding (MCF) routing protocol in Ye et al. (2001) is employed to route packets from nodes to their assigned BSs. At the Media Access Control (MAC) level, Self-organising Medium Access Control for Sensor networks (SMACS), a contention-free MAC protocol presented by Sohrabi et al. (2000) is employed to provide channel access for all the nodes. Data packets are of equal length. Each packet has 200 bits. Time axis is divided into rounds, where each round consists of 300 time frames. Each node generates one packet every 30 frames; i.e. 10 packets per round. For each network realisation in the simulation, the number of rounds it takes for the first node to die (i.e. network lifetime in number of rounds) is obtained. This lifetime averaged over several realisations of the network with 95% confidence is obtained for different number and locations of the BSs and plotted in Figure 9.

Figure 9 compares the simulated network lifetimes with the theoretical upper bounds for one, two, and three BSs. Plots for N = 50 nodes are shown. In the one BS case, the B_1 location is varied from (0, 0) to (1000, 0). The theoretical analysis predicted that the maximum lifetime bound occurs at $L/2$ (i.e. (500, 0) in this case). The simulated lifetime also is maximum at the B_1 location of (500, 0). Also, the simulated lifetime is less than the analytical upper bound. The gap between the simulated lifetime and the upper bound implies that better protocols can be devised to achieve lifetimes closer to the bound. It can be also seen that the network lifetime decreases as the node density increases (i.e. for increasing N). This is because for a fixed rate of data generation, more data need to be delivered in a round as the number of nodes increase, resulting in increased energy consumption and hence reduced network life. A similar behaviour has been reported by Hu and Li (2004). For the two BSs case, B_1 is fixed at (500, 0) and the B_2 location is varied from (0, 500) to (1000, 500). Analytical prediction is that optimum B_2 location is (500, 500). It is interesting to see that in the simulation also maximum network lifetime occurs when B_2 is located at (500, 500). In addition, for the two BSs case, the protocols employed in the simulations are found to achieve lifetimes close to the upper bound. A similar observation can be made from Figure 9 for the three BSs case also. In Figure 9, we observe that the upper bound on network life time obtained by simulation is loose by 10% for one BS, by 20% for two BSs, and by 25% for three BSs. This is mainly due the energy hole created around the BSs, an artefact of routing protocol. However, the trajectory of simulation result follows the theoretical result closely, validating the optimal BSs location precisely. Therefore, one can obtain the exact value of upper bound by placing the BSs at derived precise optimal location. In summary, the simulations validate the analytical lifetime bounds derived, and also corroborate the expected result that network lifetime can be increased by the use of multiple BSs, and more so when their locations are chosen optimally.

Figure 9 Comparison of simulated network lifetime with theoretical upper bounds. L = 1000 m, W = 500 m, N = 50 nodes, E_{battery} = 0.5 J: (a) one BS: Location of B_1 varied from (0, 0) to (1000, 0); (b) two BSs: B_1 fixed at (500,0) and location of B_2 varied from (0, 500) to (1000, 500); (c) three BSs: B_1 fixed at (500, 0), B_2 fixed at (500, 500) and B_3 varied from (0,0) to (0,500) (see online version for colours)

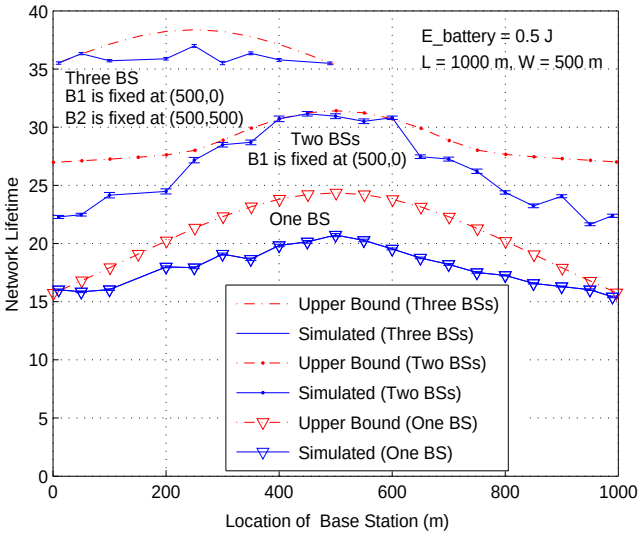

5 Conclusions

We addressed the fundamental question concerning the limits on the network lifetime in sensor networks when multiple base stations are employed as data sinks. We derived upper bounds on the network lifetime when multiple base stations are deployed along the periphery of the sensing area. We also obtained optimum locations of the base stations that maximise these network lifetime bounds. For a scenario with single base station and a rectangular region of observation, we obtained closed-form expressions for the network lifetime bound and the optimum base station location. For the case of two base stations, we jointly optimised the base station locations by maximising the lifetime bound using a GA-based optimisation. Since joint optimisation for more number of base stations is complex, for the case of three base stations, we optimised the third base station location using the previously obtained optimum locations of the first two base stations. We provided simulation results that validated the network lifetime bounds and the optimal choice of the locations of the base stations. It was shown that network lifetime can be increased by the use of multiple base stations as data sinks, more so when their locations are chosen optimally.

References

Akyildiz, I.F., Su, W., Sankarasubramaniam, Y. and Cayirci. E. (2002) 'A survey on sensor networks', *IEEE Communications Magazine*, Vol., 40, No. 8, pp.102–114.

Alsalih, W., Hassanein, H. and Akl, S. (2008) 'Placement of multiple mobile data collectors in underwater acoustic sensor networks', *Wireless Communications and Mobile Computing*, Vol. 8, No. 8, pp.1011–1022.

Arnon, S. (2005) 'Deriving an upper bound on the average operation time of a wireless sensor network', *IEEE Communications Letters*, Vol. 9, No. 2, pp.154–156.

Azad, A.K.M. and Kamruzzaman, J. (2008, May) 'A framework for collaborative multi class heterogeneous wireless sensor networks', *Proceedings of the IEEE International Conference on Communications (ICC'08)*, Beijing, pp.4396–4401.

Azad, A.P. (2006, January) *Enhancing Network Lifetime of Wireless Sensor Networks Using Multiple Base Stations and Cooperative Diversity*, Master's Thesis, Department of ECE, Indian Institute of Science, Bangalore.

Azad, A.P. and Chockalingam, A. (2006, April) 'Mobile base stations placement and energy aware routing in wireless sensor networks', *Proceedings of the Wireless Communications and Networking Conference, IEEE WCNC 2006*, Las Vegas, NV, pp.264–269.

Bhardwaj, M. and Chandrakasan, A.P. (2002) 'Bounding the lifetime of sensor networks via optimal role assignments', *Proceedings of the 21st Annual Joint Conference of the IEEE Computer and Communications Societies, IEEE INFOCOM 2002*, Vol. 3, pp.1587–1596.

Bhardwaj, M., Garnett, T., and Chandrakasan, A.P. (2001) 'Upper bounds on the lifetime of sensor networks'. *Proceedings of the IEEE International Conference on Communications*, 11–14 June, Helsinki, Finland, pp.785–790.

Blough, D.M. and Santi, P. (2002) 'Investigating upper bounds on network lifetime extension for cell-based energy conservation techniques in stationary ad hoc networks', *Proceedings of the 8th Annual International Conference on Mobile Computing and Networking, MobiCom'02*, ACM New York, NY, USA, pp.183–192.

Chandrakasan, A., Amirtharajah, R., Cho, S., Goodman, J., Konduri, G., Kulik, J., Rabiner, W. and Wang, A. (1999) 'Design considerations for distributed microsensor systems', *Proceedings of the IEEE Custom Integrated Circuits*, 16–19 May, San Diego, CA, USA, pp.279–286.

Chang, J-H. and Tassiulas, L. (2000) 'Energy conserving routing in wireless ad-hoc networks', *Proceedings of the 19th Annual Joint Conference of the IEEE Computer and Communications Societies, IEEE INFOCOM*, 26–30 March, Tel Aviv, Israel, pp.22–31.

Das, A. and Dutta, D. (2005) 'Data acquisition in multiple-sink sensor networks', *SIGMOBILE Mobile Computing and Communications Review*, Vol. 9, No. 3, pp.82–85.

Duarte-Melo, E.J., Liu, M. and Misra, A. (2004) 'A modeling framework for computing lifetime and information capacity in wireless sensor networks', *Modeling and Optimization in Mobile, Ad Hoc and Wireless Networks*, Computer Society Press.

Gandham, S.R., Dawande, M., Prakash, R. and Venkatesan, S. (2003, December) 'Energy efficient schemes for wireless sensor networks with multiple mobile base stations', *Proceedings of the IEEE Global Telecommunications Conference, GLOBECOM'03*, San Francisco, Vol. 1, pp.377–381.

Heinzelman, W. (2000) *Application-Specific Protocol Architectures for Wireless Networks*, PhD Thesis, Massachusetts Institute of Technology.

Heinzelman, W.B., Chandrakasan, A.P. and Balakrishnan, H. (2002) 'An application-specific protocol architecture for wireless microsensor networks', *IEEE Transactions on Wireless Communications*, Vol. 1, No. 4, pp.660–670.

Heinzelman, W.R., Sinha, A., Wang, A. and Chandrakasan, A.P. (2000) 'Energy-scalable algorithms and protocols for wireless microsensor networks', *IEEE International Conference on Acoustics, Speech, and Signal Processing*, 5–9 June, Istanbul, Turkey, pp.3722–3725.

Hu, Z. and Li, B. (2004, May) 'On the fundamental capacity and lifetime limits of energy-constrained wireless sensor networks', *Proceedings of the 10th IEEE Real-Time and Embedded Technology and Applications Symposium, RTAS 2004*, pp.2–9.

Kim, S., Ko, J-G., Yoon, J. and Lee, H. (2007, February) 'Multiple-objective metric for placing multiple base stations in wireless sensor networks', *Proceedings of the 2nd International Symposium on Wireless Pervasive Computing, ISWPC'07,* San Juan, pp.627–631.

Luo, H., Ye, F., Cheng, J., Lu, S. and Zhang, L. (2003) 'TTDD: two-tier data dissemination in large-scale wireless sensor networks', *Wireless Networks*, Vol. 11, pp.161–175.

Ritter, H., Schiller, J., Voigt, T., Dunkels, A. and Alonso, J. (2005) 'Experimental evaluation of lifetime bounds for wireless sensor networks', *Proceedings of the 2nd European Workshop on Wireless Sensor Networks*, 31 January–2 February, pp.25–32.

Rodoplu, V. and Meng, T.H. (1998) 'Minimum energy mobile wireless networks', *IEEE International Conference on Communications*, Vol. 3, pp.1633–1639.

Shah, R.C., Roy, S., Jain, S. and Brunette, W. (2003, May) 'Data MULEs: modeling a three-tier architecture for sparse sensor networks', *Proceedings of the 1st IEEE International Workshop on Sensor Network Protocols and Applications*, pp.30–41.

Shi, Y. and Hou, Y.T. (2009) 'Optimal base station placement in wireless sensor networks', *ACM Transactions on Sensor Networks*, Vol. 5, No.4.

Sohrabi, K., Gao, J., Ailawadhi, V. and Pottie, G.J. (2000) 'Protocols for self-organization of a wireless sensor network', *IEEE Personal Communications*, Vol. 7, No. 5, pp.16–27.

Stuber, G.L. (1997) *Principles of Mobile Communication*, Kluwer Academic Publishers, Boston, USA.

Wu, X. and Chen, G. (2007, August) 'Dual-sink: using mobile and static sinks for lifetime improvement in wireless sensor networks', *Proceedings of the 16th International Conference on Computer Communications and Networks, ICCCN'07*, Honolulu, HI, pp.1297–1302.

Xu, Y., Heidemann, J. and Estrin, D. (2001) 'Geography-informed energy conservation for ad hoc routing', *Proceedings of the 7th annual international conference on Mobile computing and networking, MobiCom'01*, ACM New York, NY, USA, pp.70–84.

Ye, F. Chen, A., Lu, S. and Zhang, L. (2001)'A scalable solution to minimum cost forwarding in large sensor networks', *Proceedings of the 10th International Conference on Computer Communications and Networks*, Scottsdale, AZ, pp.304–309.

Ye, W., Heidemann, J. and Estrin, D. (2002) 'An energy-efficient MAC protocol for wireless sensor networks', *Proceedings of the 21st Annual Joint Conference of the IEEE Computer and Communications Societies*, ACM New York, NY, USA, pp.1567–1576.

Zhang, H. and Hou, J. (2004) 'On deriving the upper bound of α-lifetime for large sensor networks', *Proceedings of the 5th ACM international symposium on Mobile ad hoc networking and computing*, *MobiHoc'04*, ACM New York, NY, USA, pp.121–132.

Zhao, W., Ammar, M. and Zegura, E. (2004) 'A message ferrying approach for data delivery in sparse mobile ad hoc networks', *Proceedings of the 5th ACM International Symposium on Mobile ad hoc Networking and Computing, MobiHoc'04*, ACM New York, NY, USA, pp.187–198.

Appendix A

In this appendix, we derive the lifetime upper bounds for the two BSs case with Same Side Orientation (SSO) and Opposite Side Orientation (OSO).

A1 Same side orientation

Consider the case of SSO shown in Figure A1. For the placement of B_1 and B_2 on the W-side, the partitioning axis Y_aY_b is represented by the straight line, where $Y_a = Y_b = (z_1 + z_2)/2$. For this SSO case, the analysis of ASO case applies with the limits (x_1, x_2), (x_3, x_4),…, (x_7, x_8) and (y_1, y_2), (y_3, y_4),…, (y_7, y_8) in the integrals in equations (31) and (32) to be $(x_3, x_4) = (y_3, y_4) = (x_7, x_8) = (y_7, y_8) = (0, 0)$, $(x_1, x_2) = (0, L)$, $(y_1, y_2) = (-z_1, (z_2 - z_1)/2)$, $(x_5, x_6) = (0, L)$, and $(y_5, y_6) = (-(z_2 - z_1)/2, W - z_2)$. Similarly, for the case of placement of B_1 and B_2 on the L-side, the partitioning axis is the line X_aX_b where $X_a = X_b = (z_1 + z_2)/2$ in Figure A1b. For this case, the limits in the integrals in equations (31) and (32) are given by $(x_3, x_4) = (y_3, y_4) = (x_7, x_8) = (y_7, y_8) = (0, 0)$, $(x_1, x_2) = (-z_1, (z_2 - z_1)/2)$, $(y_1, y_2) = (0, W)$ $(x_5, x_6) = (-(z_2 - z_1)/2, L - z_2))$, and $(y_5, y_6) = (0, W)$. Using the above, the optimum locations of BSs for SSO $(z_{1,\text{opt}}, z_{2,\text{opt}})_{\text{sso}}$ that maximises the SSO lifetime upper bound $\mathcal{T}^{(z_1,z_2)}_{\text{2-BS,sso}}$ can be computed.

Figure A1 Same side orientation (SSO) of two base stations (see online version for colours)

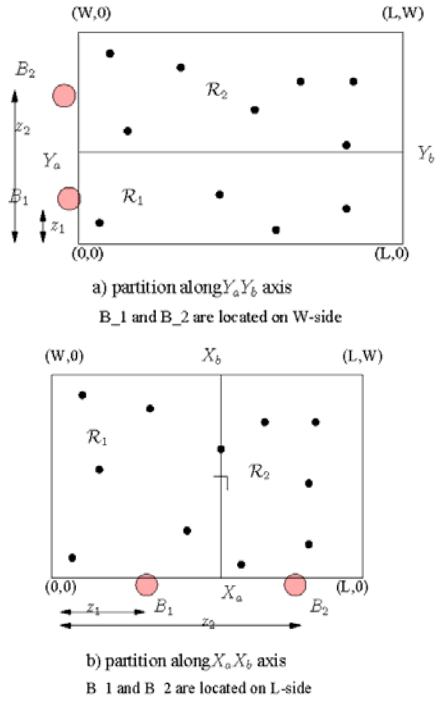

A2 Opposite side orientation

A2.1 B_1 and B_2 on the L-side

Consider the OSO case with B_1 and B_2 located on the L-side as shown in Figure A2. For a given z_1 and z_2, the partition axis will belong to any of the following possible axis types: (a) Y_aY_b, X_aY_b, Y_aX_b, and Y_aY_b when $z_1 \geq z_2$, and (b) Y_aY_b, X_aY_b, Y_aX_b, and Y_aY_b when $z_1 \leq z_2$, as shown in Figures A2(a–h). Here again, the partition axis can be represented by the straight line

$$\mathrm{Y} = mX + \mathrm{c}, \tag{A1}$$

where $m = \dfrac{z_1 - z_2}{W}$ and $c = \dfrac{W^2 - (z_1^2 - z_2^2)}{2W}$. Then, from equation (A1) we have

$$X_a = X\,|_{Y=0} \Rightarrow X_a = -\frac{c}{m} = \frac{W^2 - (z_1^2 - z_2^2)}{2(z_1 - z_2)}, \tag{A2}$$

$$X_b = \frac{W - c}{m} = \frac{W^2}{z_1 - z_2} - \frac{W^2 - (z_1^2 - z_2^2)}{2(z_1 - z_2)}, \tag{A3}$$

$$Y_a = Y\,|_{x=0} \Rightarrow Y_a = c = \frac{W^2 - (z_1^2 - z_2^2)}{2W}, \tag{A4}$$

$$Y_b = Y\,|_{X=L} \Rightarrow Y_b = mL + c = \frac{L(z_1 - z_2)}{W} + \frac{W^2 - (z_1^2 - z_2^2)}{2W}. \tag{A5}$$

For a given z_1 and z_2, $z_1 \geq z_2$, the partition axis type is

1 Y_aY_b if $Y_a \geq 0$ and $Y_b \leq W$ (Figure A2a)

2 X_aY_b if $X_a \geq 0$ and $Y_b \leq W$ (Figure A2b)

3 Y_aX_b if $Y_a \geq 0$ and $X_b \leq L$ (Figure A2c)

4 Y_aY_b if $Y_a \geq 0$ and $Y_b \leq W$ (Figure A2d),

and when $z_1 \leq z_2$, the partition axis type is

5 Y_aY_b if $Y_b \geq 0$, and $Y_a \leq W$ (Figure A2e)

6 X_bY_b if $X_a \geq 0$ and $X_b \geq 0$ (Figure A2f),

7 Y_aX_a if $Y_a \leq W$ and $X_a \leq L$ (Figure A2g)

8 X_aX_b if $X_a \leq L$ and $X_b \geq W$ (Figure A2h).

Defining $Y_{z_1} = Y\,|_{X=x+z_1}$ and $Y_{z_2} = Y\,|_{X=x+z_1} - W$ in equation (A1), the limits y_1, y_2,…, y_8 and x_1, x_2,…, x_8 in the integrals in equations (31) and (32) for the various partition axis types in Figures A2(a–d) are given in Table A1. Similarly, the limits for the partition axis types in Figures A2(e–h) are given in Table A2.

Figure A2 Different partitioning axis types for opposite side orientation (OSO) of two base stations with B_1 and B_2 on L-side (see online version for colours)

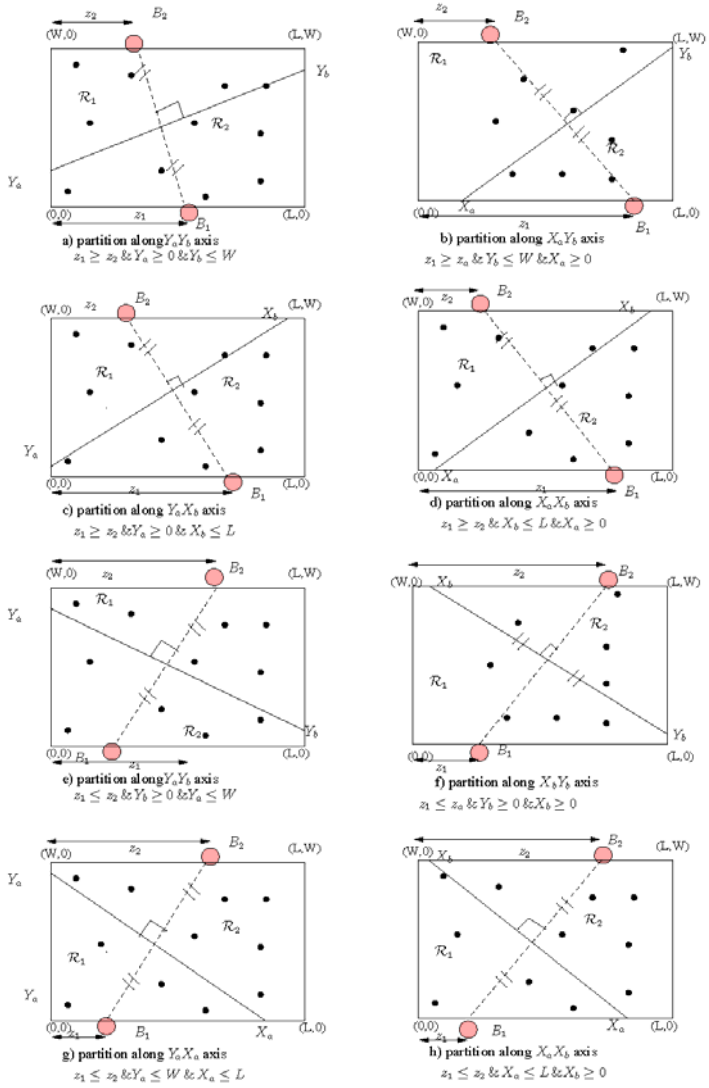

Table A1 Limits $y_1, y_2, \ldots, x_8$ in equations (31) and (32) for two base station OSO for various partition axis types in Figure A2(a-d)

Limits	*For Y_aY_b axis Figure A2a*	*For X_aY_b axis Figure A2b*	*For Y_aX_b axis Figure A2c*	*For X_aX_b axis Figure A2d*
(x_1, x_2)	$(-z_2, L-z_2)$	$(-z_2, X_a-z_2)$	$(-z_2, X_b-z_2)$	$(-z_2, X_a-z_2)$
(y_1, y_2)	$\left(0,-Y_{z_2}\right)$	$(0, W)$	$\left(0,-Y_{z_2}\right)$	$(0,W)$
(x_3, x_4)	$(0,0)$	$(X_a-z_2, L-z_2)$	$(0, 0)$	(X_a-z_2, X_b-z_2)
(y_3, y_4)	$(0,0)$	$\left(0,Y_{z_2}\right)$	$(0, 0)$	$\left(0,-Y_{z_2}\right)$
(x_5, x_6)	$(-z_1, L-z_1)$	$(X_a-z_1, L-z_1)$	$(-z_1, X_b-z_1)$	(X_a-z_1, X_b-z_1)
(y_5, y_6)	$\left(0,Y_{z_1}\right)$	$\left(0,Y_{z_1}\right)$	$\left(0,Y_{z_1}\right)$	$\left(0,Y_{z_1}\right)$
(x_7, x_8)	$(0,0)$	$(0,0)$	$(X_b-z_1, L-z_1)$	$(X_b-z_1, L-z_1)$
(y_7, y_8)	$(0,0)$	$(0,0)$	$(0, W)$	$(0, W)$

Table A2 Limits $y_1, y_2, \ldots, y_8$ and $x_1, x_2, \ldots, x_8$ in equations (31) and (32) for two base station OSO for various axis types in Figure A2(e–h)

Limits	*For Y_aY_b axis Figure A2e*	*For X_bY_b axis Figure A2f*	*For Y_aX_b axis Figure A2g*	*For X_aX_b axis Figure A2h*
(x_1, x_2)	$(-z_2, L-z_2)$	$(X_b-z_2, L-z_2)$	$(-z_2, X_a-z_2)$	(X_b-z_2, X_a-z_2)
(y_1, y_2)	$\left(0,-Y_{z_2}\right)$	$\left(0,-Y_{z_2}\right)$	$\left(0,-Y_{z_2}\right)$	$0, Y_{z_2}$
(x_3, x_4)	$(0,0)$	$(0,0)$	$(X_a-z_2, L-z_2)$	$(X_a-z_2, L-z_2)$
(y_3, y_4)	$(0,0)$	$(0,0)$	$(0, W)$	$(0, W)$
(x_5, x_6)	$(-z_1, L-z_1)$	$(-z_1, X_b-z_1)$	$(-z_1, X_b-z_1)$	$(-z_1, X_b-z_1)$
(y_5, y_6)	$(0, Yz_1)$	$(0, W)$	$0, Y_{z_1}$	$(0, L)$
(x_7, x_8)	$(0,0)$	$(X_b-z_1, L-z_1)$	$(0,0)$	(X_b-z_1, X_a-z_1)
(y_7, y_8)	$(0,0)$	$0, Y_{z_1}$	$(0,0)$	$0, Y_{z_1}$

A2.2 B_1 and B_2 on the W-side

Next, consider OSO with B_1 and B_2 located on the W-side as shown in Figure A3. For this case, the m and c in equation (A1) are given by where $m = \frac{L}{z_1 - z_2}$ and $c = \frac{(z_1^2 - z_2^2)^2 - L^2}{2(z_1 - z_2)}$, and X_a and X_b are given by

$$X_a = -\frac{(z_1^2 - z_2^2)^2 - L^2}{2L}, \tag{A6}$$

$$X_b = \frac{1}{z_1 - z_2} - \frac{(z_1^2 - z_2^2)^2 - L^2}{2L}. \tag{A7}$$

For a given z_1, z_2, the only partition axis type is X_aX_b and $X_a \geq 0$ and $X_b \geq L$ is satisfied $\forall z_1, z_2$ (Figure A3).

Defining $X_{z_1} = X|_{Y=y+z_1}$ and $X_{z_2} = Y|_{X=x+L, Y=y+z_2}$ in the X_aX_b line, the limits y_1, y_2,…, y_4 and x_1, x_2,…, x_4 in the integrals in equations (31) and (32) for this case is given by $(x_1, x_2) = (0, X_{z1})$,$(y_1, y_2) = (-z_1, W - z_1)$, $(x_3, x_4) = (0, X_{z_2})$, $(y_3, y_4) = (-z_2, W - z_2)$.

Using the above, the optimum locations of base stations for OSO $(z_{1,\text{opt}}, z_{2,\text{opt}})_{\text{oso}}$ that maximise the OSO lifetime upper bound $\mathcal{T}_{2-\text{BS,oso}}^{(z_1, z_2)}$ can be computed.

Figure A3 Opposite side orientation of two base stations with B_1 and B_2 on W-side (see online version for colours)

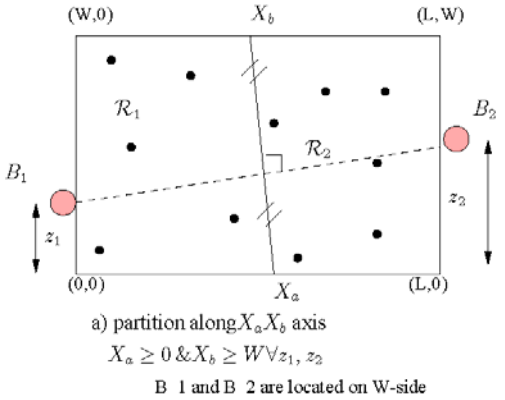

a) partition along X_aX_b axis

$X_a \geq 0 \,\&\, X_b \geq W \forall z_1, z_2$

B 1 and B 2 are located on W-side

Appendix B

In this appendix, we present the derivation of the network lifetime upper bound for the case of three BSs when $W \leq L/2$. Similar derivation can be done for the case of $L/2 < W \leq L$. As mentioned, we place BSs B_1 and B_2 in their individually optimal locations (as shown in Figure 7), and determine the optimal location of the BS B_3 that maximise the upper bound on the network lifetime. To derive the network lifetime upper bound, we need to consider two cases of placing B_3; *a*) on the adjacent side (ASO as shown in Figure 7a), and *b*) on the same side (SSO as shown in Figure 7b).

B1 Adjacent side orientation

From the solution of the two BS problem, we have the locations of B_1 and B_2 to be ($L/2$, 0) and ($L/2$, W), respectively, i.e. $z_1 = z_2 = L/2$ in Figure 7. Since B_1 and B_2 are fixed, the axes along which the partition of regions $\mathcal{R}_1$, $\mathcal{R}_2$, and $\mathcal{R}_3$ occurs depends on the location of B_3 only. Since B_3 can be placed anywhere on the W-side, we can see that $X_f \geq 0$ and $X_c \geq 0$ are always satisfied. Also, we can see that Y_b is always fixed. We have three partitioning axes (X_cX_d), (X_eX_f), (Y_aY_b) which divide the region $\mathcal{R}$ in three parts as shown in Figure 7a. Each partition axis can be represented by a straight line

$$Y = mX + c, \tag{B1}$$

where m, c for various axes are given in Table B1. Then, from equation (B1), we have

Table B1 Parameters m and c in equation (B1) for different partition axes in the three base station problem for the case of ASO

Parameter	*For Y_aY_b axis*	*For X_cX_d axis*	*For X_eX_f axis*
m	$-\frac{(z_2 - z_1)}{W}$	$\frac{z_1}{z_3}$	$\frac{z_2}{z_3 - W}$
c	$\frac{W^2 - (z_1^2 - z_2^2)}{2W}$	$\frac{(z_3^2 - k_1^2)}{2z_3}$	$\frac{z_3^2 - W^2 - z_3^2}{2(z_3 - W^2)}$

$$Y_a = Y|_{X=0} \Rightarrow Y_a = c = \frac{W^2 - (z_1^2 - z_2^2)}{2W}, \tag{B2}$$

$$Y_b = Y|_{X=L} \Rightarrow Y_b = mL + c = \frac{L(z_1 - z_2)}{W} + \frac{W^2 - (z_1^2 - z_2^2)}{2W}. \tag{B3}$$

also

$$X_c X|_{Y=0} \Rightarrow X_c = -\frac{c}{m} = -\frac{z_3^2 - z_1^2}{2z_1}, \tag{B4}$$

$$X_d = X|_{Y=W} \Rightarrow X_d = \frac{W - c}{m} = \frac{Wz_3}{z_1} - \frac{z_3^2 - z_1^2}{2z_1}, \tag{B5}$$

and

$$X_e = X|_{Y=0} \Rightarrow X_e = -\frac{c}{m} = -\frac{z_3^2 - W^2 - z_2^2}{2(z_3 - W)}, \tag{B6}$$

$$X_f = X|_{Y=W} \Rightarrow X_f = \frac{W - c}{m} = \frac{W(z_3 - W)}{z_2} - \frac{z_3^2 - W^2 - z_2^2}{2z_2}. \tag{B7}$$

Now, the energy dissipation in the entire network with BS locations z_1, z_2, and z_3 for the ASO case is given by

$$P_{\text{NW,aso}}^{(z_1,z_2,z_3)} = N\left(\iint_{\mathcal{R}_1} P_{\text{nw}}(x,y)\frac{1}{WL}dx\,dy + \iint_{\mathcal{R}_2} P_{\text{nw}}(x,y)\frac{1}{WL}dx\,dy + \iint_{\mathcal{R}_3} P_{\text{nw}}(x,y)\frac{1}{WL}dx\,dy\right). \tag{B8}$$

By the minimum energy relay argument, we have $P_{\text{nw}}(x,y) \geq P_{\text{link}}\left(\sqrt{x^2 + y^2}\right)$, where $P_{\text{link}}(D)$ is given by equation (7). Hence,

$$\begin{aligned} P_{\text{NW,aso}}^{(z_1,z_2,z_3)} &\geq \frac{N}{WL}\left(\iint_{\mathcal{R}_1} P_{\text{link}}(\sqrt{x^2+y^2})\,dx\,dy + \iint_{\mathcal{R}_2} P_{\text{link}}(\sqrt{x^2+y^2})\,dx\,dy + \iint_{\mathcal{R}_3} P_{\text{link}}(\sqrt{x^2+y^2})\,dx\,dy\right) \\ &\geq \frac{r\alpha_1}{d_{\text{char}}}\frac{\eta}{\eta - 1}\frac{N}{WL}\left(+\iint_{\mathcal{R}_1}\sqrt{x^2+y^2})\,dx\,dy + \iint_{\mathcal{R}_2}(\sqrt{x^2+y^2})\,dx\,dy + \iint_{\mathcal{R}_3}(\sqrt{x^2+y^2})\,dx\,dy\right) \\ &\geq \frac{r\alpha_1}{d_{\text{char}}}\frac{\eta}{\eta - 1}\frac{N}{WL}\left[d_{3-BS,aso}^{\mathcal{R}_1}(z_1,z_2,z_3) + d_{3-\text{BS,aso}}^{\mathcal{R}_2}(z_1,z_2,z_3) + d_{3-\text{BS,aso}}^{\mathcal{R}_3}(z_1,z_2,z_3)\right], \end{aligned} \tag{B9}$$

where $d_{3-\text{BS,aso}}^{\mathcal{R}_1}(z_1,z_2,z_3)$, $d_{3-\text{BS,aso}}^{\mathcal{R}_2}(z_1,z_2,z_3)$ and $d_{3-\text{BS,aso}}^{\mathcal{R}_3}(z_1,z_2,z_3)$ are of the form

$$d_{3-\text{BS,aso}}^{\mathcal{R}_1}(z_1,z_2,z_3) = \int_{y_1}^{y_2}\int_{x_1}^{x_2}\sqrt{x^2+y^2}\,dx\,dy + \int_{y_3}^{y_4}\int_{x_3}^{x_4}\sqrt{x^2+y^2}\,dx\,dy, \tag{B10}$$

$$d_{3-\text{BS,aso}}^{\mathcal{R}_2}(z_1,z_2,z_3) = \int_{x_5}^{x_6}\int_{y_5}^{y_6}\sqrt{x^2+y^2}\,dy\,dx + \int_{x_7}^{x_8}\int_{y_7}^{y_8}\sqrt{x^2+y^2}\,dy\,dx, \tag{B11}$$

and

$$d_{3-\text{BS,aso}}^{\mathcal{R}_2}(z_1,z_2,z_3) = \int_{x_9}^{x_{10}}\int_{y_9}^{y_{10}}\sqrt{x^2+y^2}\,dy\,dx + \int_{x_{11}}^{x_{12}}\int_{y_{11}}^{y_{12}}\sqrt{x^2+y^2}\,dy\,dx, \tag{B12}$$

Now, denoting (X_I, Y_I) to be the coordinates of the point of intersection of the three axes Y_aY_b, X_cX_d and X_eX_f, we have

$$X_I = \frac{c_2 - c_1}{m_1 - m_2}, \quad Y_1 = \frac{c_1 m_2 - c_2 m_1}{m_2 - m_1}, \tag{B13}$$

where m_1, c_1 and m_2, c_2 are the m, c parameters for the Y_aY_b and X_cX_d axes, respectively, as given in Table B1. Also, define

$Y_{l_1 z_2} = Y|_{X=x+z_2} - W$ and $Y_{l_1 z_1} = Y|_{X=x+z_1}$ in the Y_aY_b line,

$X_{l_2z_3} = X|_{Y=y+z_3}$ and $Y_{l_2z_1} = Y|_{X=x+z_1}$ in the X_cX_d line, and

$X_{l_3z_3} = X|_{Y=y+z_3}$ and $Y_{l_3z_2} = Y|_{X=x+z_2} - W$ in the X_eX_f line.

Using the above definitions, we can write the limits of the integrals in equations (B10)–(B12) to be as given in Table B2.

Table B2 Limits $y_1, y_2, \ldots, y_{12}$ and $x_1, x_2, \ldots, x_{12}$ in the integrals in equations (B10)–(B12) in the three base station problem for the case of ASO

Limits		*Values*	
(x_1, x_2)	(y_1, y_2)	$(0, X_{l_2z_3})$	$(-z_3, Y_1 - z_3)$
(x_3, x_4)	(y_3, y_4)	$(0, X_{l_3z_3})$	$(Y_1 - z_3, W - z_3)$
(x_5, x_6)	(y_5, y_6)	$(X_f - z_2, X_1 - z_2)$	$(0, -Y_{l_3z_2})$
(x_7, x_8)	(y_7, y_8)	$(X_1 - z_2, L - z_2)$	$(0, -Y_{l_1z_2})$
(x_9, x_{10})	(y_9, y_{10})	$(X_c - z_1, X_1 - z_1)$	$(0, Y_{l_2z_1})$
(x_{11}, x_{12})	(y_{11}, y_{12})	$(X_1 - z_1, L - z_1)$	$(0, Y_{l_1z_1})$

Now, denoting $\mathcal{T}_{\text{3-BS,aso}}^{(z_1,z_2,z_3)}$ as the network lifetime with three BSs at locations z_1, z_2, z_3 for the ASO case, we have

$$P_{\text{NW,aso}}^{(z_1,z_2,z_3)} \mathcal{T}_{\text{3-BS,aso}}^{(z_1,z_2,z_3)} \le NE_{\text{battery}}. \tag{B14}$$

Hence, an upper bound on the network lifetime for a given (z_1, z_2, z_3) for the case of ASO can be obtained as

$$\mathcal{T}_{\text{3-BS,aso}}^{(z_1,z_2,z_3)} \le \frac{NE_{battery}}{\frac{r\alpha_1}{d_{\text{char}}} \frac{\eta}{\eta - 1} \frac{N}{WL} A(z_1, z_2, z_3)}.$$

where

$$A(z_1, z_2, z_3) = d_{\text{3-BS,aso}}^{\mathcal{R}_1}(z_1, z_2, z_3) + d_{\text{3-BS,aso}}^{\mathcal{R}_2}(z_1, z_2, z_3) d_{\text{3-BS,aso}}^{\mathcal{R}_3}(z_1, z_2, z_3).$$

The optimum BS locations for the ASO case that maximises the above lifetime bound is then given by

$$\left(z_{3,\text{opt}}\right)_{\text{aso}} = \underset{z_3 \in (0,W)}{\arg\max}\ \mathcal{T}_{\text{3-BS,aso}}^{(z_1,z_2,z_3)}. \tag{B15}$$

B2 Same side orientation

A similar approach can be adopted for the case of SSO of the placement of B_3 as shown in Figure 7b. Here, the region $\mathcal{R}$ can be divided into $\mathcal{R}_1$, $\mathcal{R}_2$, and $\mathcal{R}_3$ using the partitioning axes Y_aY_b, X_cX_d, and X_eY_e, as shown in Figure 7b. The m and c parameters for these three axes are given in Table B3. Also, the limits in the integrals of equations (B10)–(B12) for the case of SSO are given in Table B4, where

$Y_{l_1z_2} = Y|_{X=x+z_2} - W$ and $Y_{l_1z_1} = Y|_{X=x+z_1}$ in the Y_aY_b line, and

$Y_{l_3z_3} = Y|_{X=x+z_3}$ and $Y_{l_3z_2} = Y|_{X=x+z_2} - W$ in the Y_eY_e line,

Table B3 Parameters m and c in equation (B1) for different partition axes in the three base station problem for the case of SSO

Parameter	*For Y_aY_b axis*	*For X_cX_d axis*	*For X_eX_e axis*
m	$-\frac{(z_2 - z_1)}{W}$	∞	$-\frac{z_2 - z_3}{W}$
c	$\frac{W^2 + z_2^2 - z_1^2}{2W}$	$-\infty$	$\frac{W^2 + (z_2 - z_3)(z_1 + z_3)}{2(z_3 - z^2)}$

Table B4 Limit $y_1, y_2, \ldots, y_{12}$ and $x_1, x_2, \ldots, x_{12}$ in the integrals in equations (B10)–(B12) in the three base station problem for the case of SSO

Limits		*Values*	
(x_1, x_2)	(y_1, y_2)	$(-z_3, X_c - z_3)$	$\left(0, Y_{l_3z_3}\right)$
(x_3, x_4)	(y_3, y_4)	$(0,0)$	$(0,0)$
(x_5, x_6)	(y_5, y_6)	$(-z_2, X_c - z_2)$	$\left(0, -Y_{l_3z_2}\right)$
(x_7, x_8)	(y_7, y_8)	$(X_c - z_2, L - z_2)$	$\left(0, -Y_{l_1z_2}\right)$
(x_9, x_{10})	(y_9, y_{10})	$(X_c - z_1, L - z_1)$	$\left(0, Y_{l_1z_1}\right)$
(x_{11}, x_{12})	(x_{11}, x_{12})	$(0,0)$	$(0,0)$

Using the values in Tables B3 and B4, and following similar steps as in the case of ASO, the optimum location of B_3 for the case of SSO can be found as

$$\left(z_{3,\text{opt}}\right)_{\text{sso}} = \underset{z_3 \in (0,W)}{\arg\max}\ \mathcal{T}_{\text{3-BS,sso}}^{(z_1,z_2,z_3)}. \tag{B16}$$